

# Australian east coast rainfall decline related to large scale climate drivers

Milton Samuel Speer · Lance M. Leslie ·  
Alexandre O. Fierro

Received: 23 August 2009 / Accepted: 9 December 2009 / Published online: 31 December 2009  
© Springer-Verlag 2009

**Abstract** Rainfall on the subtropical east coast of Australia has declined at up to 50 mm per decade since 1970. Wavelet analysis is used to investigate eight station and four station-averaged rainfall distributions along Australia's subtropical east coast with respect to the El Niño-Southern Oscillation (ENSO), the inter-decadal Pacific oscillation (IPO) and the southern annular mode (SAM). The relationships are examined further using composite atmospheric circulation anomalies. Here we show that the greatest rainfall variability occurs in the 15–30 year periodicity of the 1948–1975 or ‘cool’ phase of the IPO when the subtropical ridge is located sufficiently poleward for anomalous moist onshore airflow to occur together with high ENSO rainfall variability and high, negative phase, SAM variability. Thus, the mid-latitude westerlies are located at their most equatorward position

in the Australian region. This maximizes tropospheric interaction of warm, moist tropical air with enhanced local baroclinicity over the east coast, and hence rainfall.

**Keywords** Rainfall variability · Large scale · Climate drivers · East Australia

## 1 Introduction

Eastern Australia, particularly along the subtropical coast ( $25^{\circ}\text{S}$ – $38^{\circ}\text{S}$ ) where approximately 50% of Australia's population inhabits about 5% of its total land area, has experienced a decline in rainfall over the latter half of the twentieth century at a rate of between 30 and 50 mm per decade and 40–50 mm per decade since 1970 (Fig. 1a, b). The recent eastern Australian severe drought (2002–2007) has placed increasing pressure on water resource availability (Murphy and Timbal 2008). The El Niño of 2006/2007 exacerbated the drought and along with the 2002/2003 El Niño produced a 5-year drought that was the worst reported over the last century (Bureau of Meteorology 2006).

From an Australian perspective, identifying the likely causes for the decline in rainfall on the east coast during the latter half of the twentieth century, and during the last decade in particular, is considered the highest priority for new detection and attribution studies because of the large population and high economic value of the region (Nicholls 2006). Various studies have investigated the relationship between rainfall over Australia and large scale climate drivers (McBride and Nicholls 1983; Stone and Auliciems 1992; Zhang and Casey 1992; Nicholls and Kariko 1993; Cordery and Opoku-Ankomah 1994), especially in relation to the El Niño-Southern Oscillation (ENSO) phenomenon. The southern oscillation index (SOI) is defined as the

**Electronic supplementary material** The online version of this article (doi:[10.1007/s00382-009-0726-1](https://doi.org/10.1007/s00382-009-0726-1)) contains supplementary material, which is available to authorized users.

M. S. Speer (✉)  
Faculty of Science, Climate Change Research Centre,  
The University of New South Wales, Level 4,  
Matthews Building, Sydney 2052, Australia  
e-mail: milton.speer@unsw.edu.au

L. M. Leslie  
Cooperative Institute for Mesoscale Meteorological Studies  
and School of Meteorology, The University of Oklahoma,  
Norman, OK, USA

L. M. Leslie  
Australian Sustainable Development Institute,  
Curtin University, Perth, Australia

A. O. Fierro  
NOAA/Hurricane Research Division,  
Atlantic Oceanographic Meteorological Laboratory,  
Miami, FL, USA

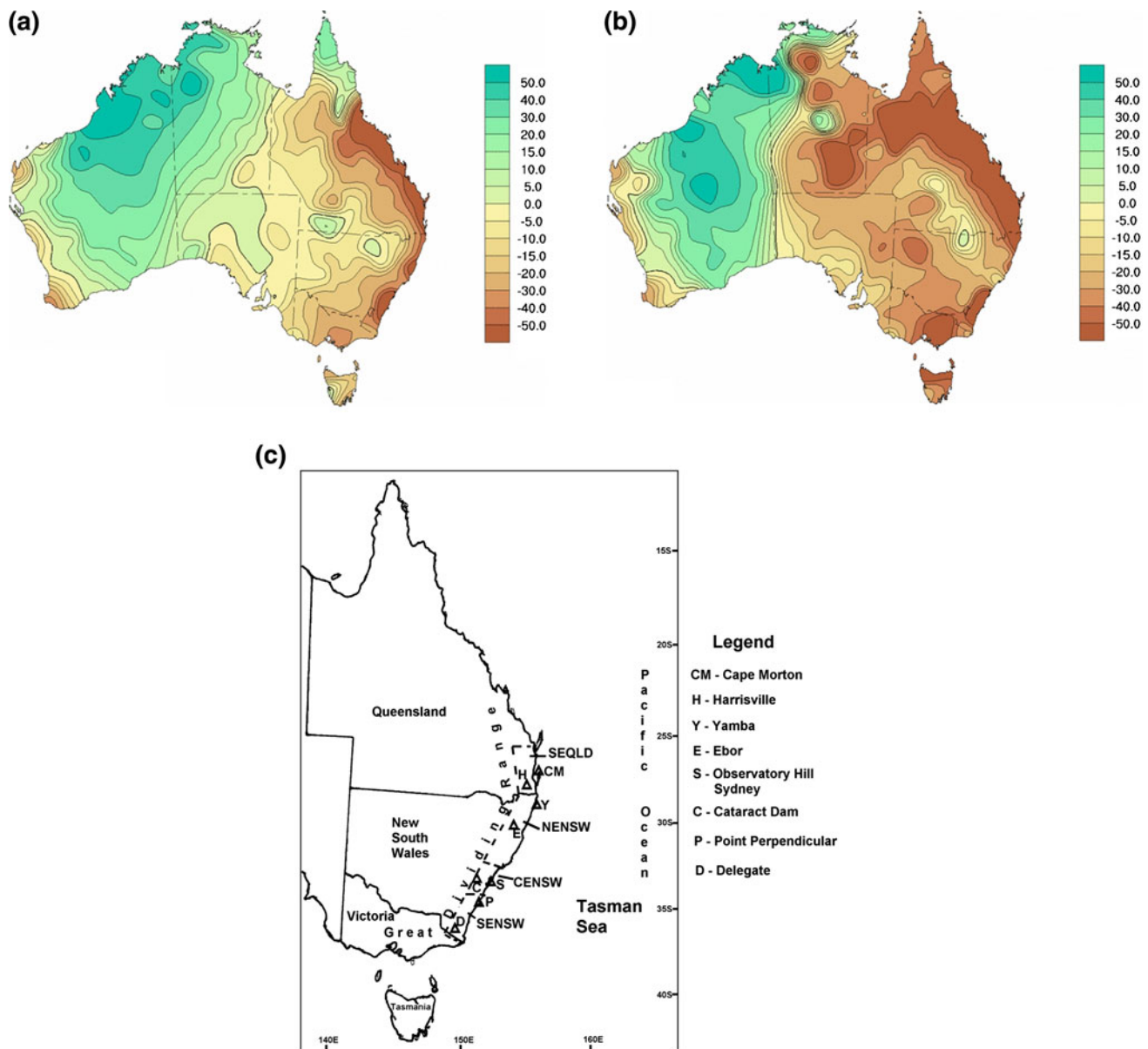


**Fig. 1** Map of Australia highlighting the decline in annual rainfall (mm/10 years) along the east coast from, (a) 1950–2007, and (b) as in (a), except for 1970–2007, (c) Map of eastern Australia highlighting features mentioned in the text including the four study regions of southeast Queensland (SEQLD), and northeast, central eastern and southeastern New South Wales (NENSW, CENSW, and SENSW,

respectively). Also, within each region two rainfall stations are indicated with reference to wavelet analysis figures presented later. The rainfall stations are: CM Cape Morton, H Harrisville (SEQLD), Y Yamba, E Ebor (NENSW), S Observatory Hill, C Cataract (CENSW), P Point Perpendicular, D Delegate (SENSW) (Please refer ESM for original higher-resolution figures)

normalized monthly Tahiti minus Darwin pressure difference and hence is a measure of the strength of the Walker circulation. Sustained high negative/positive values indicate El Niño/La Niña conditions. Ansell et al. (2000) investigated evidence for decadal variability in southern Australian rainfall and relationships with regional pressure and sea-surface temperature (SST). Hendon et al. (2007) and Meneghini et al. (2007) investigated the effect of the southern annular mode (SAM) on Australian rainfall and atmospheric circulation. The SAM is the leading mode of

variability in the extra-tropical southern hemispheric circulation and is characterized by deep, zonally symmetric or “annular” structures, with geopotential height perturbations of opposing signs in the polar cap region and in the surrounding zonal ring centered near 45°S (Thompson and Wallace 2000). The SAM index is defined as the difference in the normalized monthly zonal mean sea level pressure (MSLP) between 40°S and 70°S (Nan and Li 2003). Ummenhofer et al. (2009) related severe droughts in the State of Victoria (see Fig. 1c) to the Indian Ocean dipole.

However, with the three preceding studies (Hendon et al. 2007; Meneghini et al. 2007; Ummenhofer et al. 2009), the predominant focus has been south of about 35°S (i.e., the southwest and southeast corners of the continent) and the tropical north, or generally Australia-wide, and none of those studies have included the inter-decadal Pacific oscillation (IPO). The IPO is used to describe the Pacific wide ENSO-like pattern of SST that emerged in the analysis of near-global inter-decadal SST (Folland et al. 1999). Power et al. (2006) showed that the IPO can appear to modulate ENSO activity and ENSO's impact on Australia's climate including rainfall, even if the IPO largely reflects unpredictable random changes in the relative frequency of El Niño and La Niña events in a given inter-decadal period. Power et al. (1999) found that when the IPO raises temperatures in the tropical Pacific Ocean there is no robust relationship between year-to-year Australian climate variations and ENSO. On the other hand, when the IPO lowers temperatures in the same region, they concluded that year-to-year ENSO variability is closely associated with year-to-year Australian rainfall variability. Pezza et al. (2007) found that trends in the closely related Pacific decadal oscillation (PDO) observed over the Tasman Sea are consistent with declining winter rainfall over southeastern Australia. The PDO is the predominant source of inter-decadal climate variability in the Pacific Northwest and is characterized by changes in sea surface temperature, sea level pressure, and wind patterns (Zhang et al. 1997; Mantua et al. 1997). Rakich et al. (2008) examined aspects of the influence of both the SAM and ENSO on New South Wales (NSW) rainfall and found that SAM predominantly influences southern NSW rainfall while ENSO predominantly influences northern NSW rainfall. Speer (2008) related a sharp decrease in NSW coastal rain producing systems in the mid-1970s to a reversal in phase of the IPO and concluded a further decrease from the mid-1990s most likely due to an increasingly positive SAM.

In summary, to investigate the reasons for the decline in rainfall over the subtropical Australian east coast, three large scale climate drivers consisting of the IPO, SAM and SOI are used to study Australian subtropical east coast rainfall variability in an area defined by the coastal strip between 25°S and 38°S. This area is further divided into four sections: southeast Queensland (SEQLD), northeast New South Wales (NENSW), central east New South Wales (CENSW) and southeast New South Wales (SENSW) (see Fig. 1c). The rationale for the divisions follows from SEQLD having a predominantly annual wet/dry season regime while for the three NSW divisions, the influence of tropical weather systems decreases southward and the mid-latitude weather system influence decreases northward. Finally, rainfall variability for one coastal and one inland station within each of the four areas is also analyzed since annual rainfall decreases inland.

## 2 Data and methodology

### 2.1 Data

The station monthly rainfall time series in this study were developed from a high quality rainfall dataset highly suited for monitoring long-term trends and variability in Australian rainfall (Jones and Weymouth 1997; Lavery et al. 1997). The area-averaged rainfall for each of the four regions is simply the average of the high quality rainfall station data used within each of the four regions (Table 1). That enabled at least one coastal and one inland rainfall station to be included for each of the four regions (see Fig. 1c). The coastal station of Observatory Hill is not a high quality station as defined by Lavery et al. (1997). However, it was included in CENSW owing to a lack of high quality coastal station rainfall data in CENSW and is considered satisfactory for analyzing seasonal and annual rainfall. The IPO monthly time series are reanalyzed values using the improved HadSST2 data (Rayner et al. 2006) by Parker et al. (2007). The SAM monthly data are obtained from: (<http://www.lasg.ac.cn/staff/ljp/data-NAM-SAM-NAO/SAM-AAO.htm#>) and are originally based on work by (Nan and Li 2003). Monthly values of the SOI which represent the difference in MSLP between Tahiti and Darwin standardized to a mean of zero and a standard deviation of 10, were provided by the National Climate Centre of the Australian Bureau of Meteorology. Composite atmospheric circulation anomalies are derived from NCEP reanalysis data (Kalnay et al. 1996) and the plots are provided by the NOAA/ESRL Physical Sciences Division, Boulder Colorado from their web site at <http://www.cdc.noaa.gov/>. There are several reanalysis schemes in widespread use for studying decadal variations and arguments can be made for choosing a particular reanalysis data set. Chen et al. (2008) use both ERA40 and NCEP reanalysis schemes to study the spatio-temporal structure of twentieth century climate variations in observations and reanalyses. However, in this study we chose the NCEP reanalysis data, especially given that Hope (2005) found the quality of these data to be appropriate for defining trends in atmospheric pressure over Australia.

### 2.2 Wavelet analysis

Wavelet transform analysis examines a time series using generalized local base functions (mother wavelets) that are stretched and translated with a resolution in both frequency and time. The wavelets can be used to analyze non-stationary time series and give a distribution of power in two dimensions, namely, time and frequency rather than just the one dimension of frequency, as in Fourier analysis. Therefore, wavelet transform analysis provides information on both the amplitude of a periodic signal within a time series and how the amplitude varies with time including

**Table 1** Rainfall station names along with their latitude/longitude and altitude above sea-level for which Australian Bureau of Meteorology archived rainfall data was used in the area-averaging for the four study regions

Station name	Latitude/longitude (degree)	Altitude (m)	Region
Cowal	25.82S 152.62E	61	SEQLD (inland)
Beaudesert	28.00S 152.99E	46	SEQLD (inland)
Cape Morton Lighthouse	27.03S 153.47E	100	SEQLD (coast)
University of Queensland Gatton	27.55S 152.34E	94	SEQLD (inland)
Harrisville Post Office	27.81S 152.67E	55	SEQLD (inland)
Yamba Pilot Station	29.43S 153.36E	29	NENSW (coast)
Casino Airport	28.88S 153.05E	26	NENSW (inland)
Ebor	30.37S 152.40E	1270	NENSW (inland)
Port Macquarie	31.44S 152.92E	7	NENSW (coast)
Stroud Post Office	32.41S 151.97E	44	NENSW (inland)
Branxton	32.64S 151.42E	30	CENSW (inland)
Cataract Dam	34.27S 150.81E	340	CENSW (inland)
Observatory Hill Sydney	33.86S 151.20E	40	CENSW (coast)
Point Perpendicular Lighthouse	35.09S 150.80E	85	SENSW (coast)
Bettowyd	35.72S 150.15E	165	SENSW (inland)
Moruya Heads Pilot Station	35.91S 150.15E	17	SENSW (coast)
Delegate	37.05S 148.99E	750	SENSW (inland)

trends, breakdown points and discontinuities (Torrence and Compo 1998). There are many reviews on the theoretical aspects of wavelet and Fourier transform in the literature (e.g., Foufoula-Georgiou and Kumar 1995; Lau and Wen 1995; Torrence and Webster 1999). In this study, as in Torrence and Webster (1999), we use the well-known Morlet wave (Morlet 1982) which consists of a plane wave modified by a Gaussian envelope and can be represented as,  $e^{i\omega_0 t} e^{-t^2/(2s^2)}$ , where  $t$  is the time,  $s$  is the wavelet scale, and  $\omega_0$  is a non-dimensional frequency. For  $\omega_0 = 6$  (used here), there are approximately three oscillations within the Gaussian envelope.

The wavelet power spectrum is defined as the absolute value squared of the wavelet transform and gives a measure of the time series variance at each scale (period) and at each time. The transform on the Morlet wave is performed in Fourier space using the method described in Torrence and Compo (1998) in which the wavelet transform conserves variance. According to Kestin et al. (1998), in order to test for non-stationary changes in variance, it is most appropriate to choose the global wavelet spectrum (GWS), given by the time average of the wavelet power spectrum.

### 3 Results

#### 3.1 Periodicity of rainfall and the three climate drivers

The wavelet power spectra for the IPO, SAM, SOI, the four area-averaged rainfall regions and two individual rainfall

stations (one coastal and one inland) for each of the four east Australian coastal regions, are shown in Figs. 2a–c, 3a–d and 4a–h, respectively. In each figure, the top panel represents the monthly time series, the bottom left panel represents the wavelet spectrum with cone of influence (dashed, black contour), and the bottom right panel shows the GWS which highlights the power or strength of the periodicity with respect to the total power within the time period selected.

#### 3.2 Annual periodicity

The three northern-most area-averaged rainfall regions SEQLD (Fig. 3a), NENSW (Fig. 3b) and CENSW (Fig. 3d) show high variability in their wavelet spectra for the annual cycle with periods of high variability decreasing poleward, as expected, since the northern most region, SEQLD, being located closer to the tropics, has predominantly a wet/dry annual cycle. This decreasing annual cycle influence in the four regions from north to south is also evident in the wavelet spectra for individual stations discussed in the following paragraph.

The annual cycle is the dominant periodicity of high rainfall variability for the inland stations in SEQLD (see Fig. 4a) and NENSW (see Fig. 4c) while the coastal stations of Cape Morton (Fig. 4b) in SEQLD, Yamba (Fig. 4d) in NENSW and Observatory Hill (Fig. 4f) in CENSW also exhibit high annual rainfall variability. This is not surprising as these two northern-most regions are close to the wet/dry annual rainfall regime of the tropics.

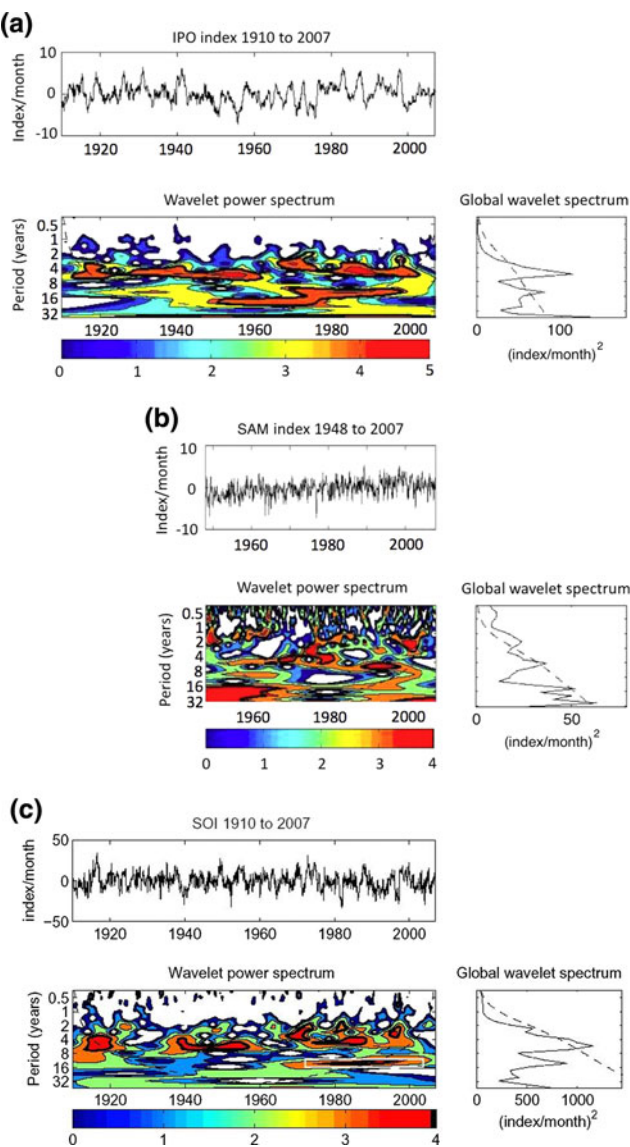


**Fig. 2** (a) IPO monthly index values from 1910 to 2007 (top); wavelet power spectrum indicating periods ranging from low (dark blue) to high (red) IPO variability (bottom left). High variability periods specifically mentioned in the text are indicated by the enclosed area within a white rectangle; and, global wavelet spectrum highlighting the power (or intensity) of IPO variability (bottom right). The power is defined as  $(\text{index})^2$  and is indicated on the x-axis. The 5% level of significance in variance is also shown in the bottom left panel by the areas enclosed within the thick, black contour lines (solid), and as the dashed line in the GWS in the bottom, right panel, (b) as in (a), except for the SAM index from 1948 to 2007, (c) as in (a), except for the SOI (Please refer ESM for original higher-resolution figures)

Further south, a transition is evident to diminishing high rainfall variability in the annual cycle for the CENSW inland station of Cataract (Fig. 4e) and in SENSW the annual cycle is also diminished in importance for both the coastal station of Point Perpendicular (Fig. 4h) and the inland station of Delegate (Fig. 4g).

### 3.3 2–7 year (ENSO) periodicity

For the 2–7 year periodicity, two high rainfall variability periods are evident from 1915 to 1925 and the 1950s to 1960s in three of the area-averaged rainfall regions consisting of SEQLD, NENSW and CENSW while for SENSW (Fig. 3d) there is also a third high rainfall variability period from the late 1960s to the mid-1980s. While 2–7 year rainfall variance in the four area-averaged regions closely matches that in the SOI wavelet spectrum, the most striking feature is that it is weaker in the four regions and is *not* significant at the 5% level as shown in their GWSs compared to the SOI, where it *is* significant at the 5% level as indicated in the SOI GWS. This reflects the low association of NSW coastal rainfall with the SOI (McBride and Nicholls 1983; Bureau of Meteorology 2005).

The 2–7 year periodicity for the individual stations in each of the four regions broadly matches that for each area-averaged region, although the three periods shown for the coastal station of Point Perpendicular in SENSW (Fig. 4h), have much weaker power than the inland station of Delegate (Fig. 4g).

### 3.4 15–30 year periodicity

We now concentrate on inter-decadal periodicity to provide a framework for comparing multi-decadal composite anomalies of atmospheric circulation re-analyses.

The 15–30 year periodicity in the IPO, SAM, SOI and the four area-averaged rainfall regions shows large changes in variability since 1910. There is high variability (though not statistically significant at the 5% level) for the two northern-most rainfall regions (SEQLD and NENSW) from 1920 to the mid-1970s and for CENSW from 1920 to the 2007, which is statistically significant at the 5% level. For the IPO there is high 20–30 year variability from the late 1940s to the mid-1970s. This period contains the four highest annual rainfall totals for eastern Australia including the State of NSW (Fig. 5a, b). The SAM shows high 20–30 year variability in its negative phase in the 1950s and from the mid-1990s in its positive phase (see Fig. 2b). SAM positive values are associated with reduced rainfall over southeastern Australia (Nicholls 2009). These changes in the IPO and SAM are the main reason that extreme annual rainfall totals over eastern Australia have decreased since the mid-1970s (Speer 2008) and it is the decline along the subtropical east coast ( $25^\circ\text{S}$ – $38^\circ\text{S}$ ) (Figs. 5a, b), that is the area of interest in this study. Sustained periods of large negative SOI values indicate El Niño or drought conditions over eastern Australia and the SOI indicates high variability from 1970 to 2007 (Fig. 2c).

The highest 15–30 year rainfall variability for SENSW starts about the late 1940s with the ‘cool’ or negative phase

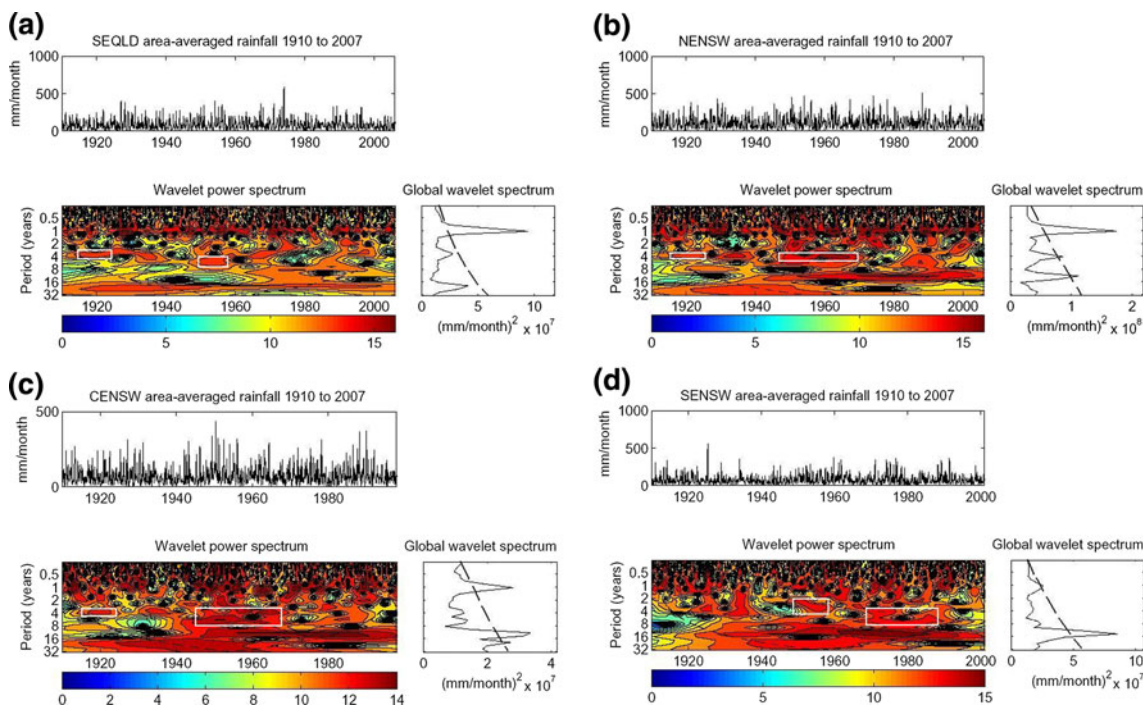


**Fig. 3** (a) SEQLD area-averaged monthly rainfall (mm) from 1910 to 2007—(top); wavelet power spectrum indicating periods ranging from low (dark blue) to high (red) rainfall variability (bottom left). High variability periods specifically mentioned in the text are indicated by the area enclosed within a white rectangle; and, global wavelet spectrum highlighting the power or intensity of rainfall variability (bottom right).

The power is defined as,  $(\text{mm/month})^2$  and is indicated on the *x*-axis. The 5% significance level in variance is also shown in the *bottom left panel* by the areas enclosed within the *thick, black contour lines (solid)*, and as the *dashed line* in the GWS in the *bottom, right panel*, (b) as in (a), except for NENSW, (c) as in (a), except for CENSW, (d) as in (a) except for SENSW (Please refer ESM for original higher-resolution figures)

of the IPO and continues through the negative to positive IPO phase into the mid-1990s. While SEQLD and NENSW 15–30 year high rainfall variability periods occur from 1920 to the mid-1970s, there is less power in their respective global wavelet spectra than SENSW and CENSW. This implies that the 15–30 year periodicity prior to the mid-1970s is more significant for attributing higher rainfall over this period in SENSW and CENSW than in NENSW and SEQLD. The reason for these differences in rainfall variability between the two southern regions and two northern regions are discussed in the next section in relation to atmospheric circulation anomalies.

### 3.5 Atmospheric circulation anomalies

In the following IPO, SAM and SOI wavelet diagrams high  $\pm$  variability periods imply that atmospheric circulation regimes associated with those respective  $\pm$  phases may dominate in certain regions. In the rainfall wavelet diagrams, high rainfall variability periods are manifested in the annual time series as periods in which typically there are larger annual rainfall totals than periods with low rainfall variability. Changes from high (low) to low (high) rainfall variability periods for a given location or region

may imply changes in atmospheric circulation regimes affecting that area or location.

Salinger et al. (2001) showed that the mid-1970s was a pivotal period for New Zealand circulation, temperature and precipitation trends, when the sub-tropical ridge shifted north such that MSLP anomalies covered the region west of 170°W to the Australian east coast. The positive anomalies replaced negative MSLP anomalies in the same area which they attributed to a change in phase of the IPO. As mentioned in the previous sub-section, the decline in rainfall over the subtropical east coast is related to the IPO phase shift from negative to positive in the mid-1970s. Typically, during the 1948–1975 negative phase IPO the subtropical ridge is located anomalously poleward and in the 1976–1998 positive IPO phase it is located anomalously equatorward (see Fig. 6a compared to Fig. 7a). This has the effect of enhancing onshore airflow and available moisture over the east coast in the negative phase while favouring offshore airflow and thereby minimizing available moisture advection over the east coast in the 1976–1998 positive IPO phase.

Composite atmospheric circulation anomalies for the two IPO phases 1948–1975 and 1976–1998 are shown in Figs. 6a–d and 7a–d, respectively. Furthermore, in the

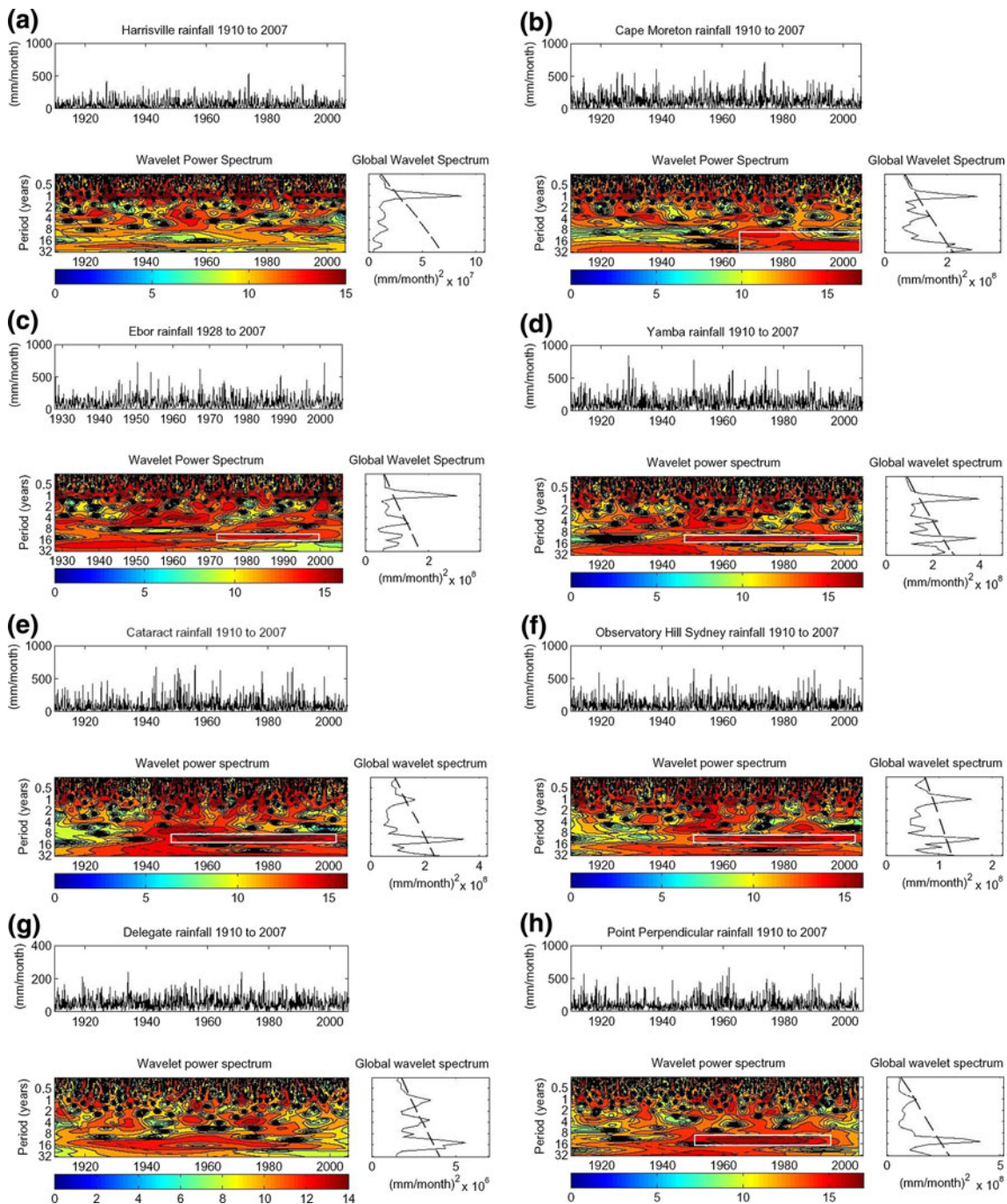


**Fig. 4** (a) Harrisville monthly rainfall (mm) from 1910 to 2007 (*top*); wavelet power spectrum indicating periods ranging from low (*dark blue*) to high (*red*) rainfall variability (*bottom left*). High variability periods specifically mentioned in the text are indicated by the area enclosed within a *white rectangle*; and global wavelet spectrum highlighting the power or intensity of rainfall variability (*bottom right*). The power is defined as  $(\text{mm/month})^2$  and is indicated on the *x*-axis. The 5% significance level in variance is also shown in the

*bottom left panel* by the areas enclosed within the *thick, black contour lines (solid)*, and as the *dashed line* in the GWS in the *bottom, right panel*, (b) as in (a), except for Cape Morton, (c) as in (a), except for Ebor from 1928 to 2007, (d) as in (a), except for Yamba, (e) as in (a), except for Cataract, (f) as in (a), except for Observatory Hill Sydney, (g) as in (a), except for Delegate, (h) as in (a), except for Point Perpendicular (Please refer ESM for original higher-resolution figures)

period 1948–1975 negative MSLP anomalies over north-east Australia and negative 300 hPa anomalies in the mid-latitudes and tropics (Fig. 6a, b) are indicative of a period

in which mid-latitude/tropical tropospheric interactions occurred. This can be explained from the work of Codron (2005, 2007) and more recently Kidston et al. (2009).

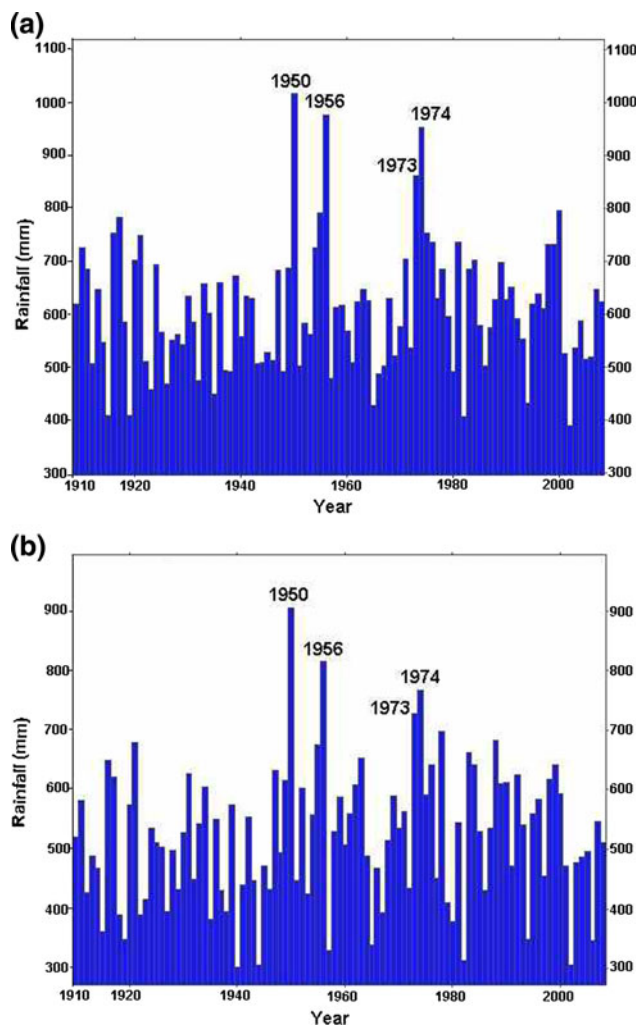


**Fig. 5** Annual rainfall 1910–2007 highlighting the four highest rainfall years in the 1948–1975 period for, (a) eastern Australia (defined by BoM as including the States of Queensland, New South Wales, Victoria and Tasmania—see Fig. 1c), and (b), as in (a), except for the State of New South Wales

Kidston et al. conclude that when the SAM is in its negative phase the mid-latitude polar jet stream wind speed anomalies are weaker in eastern Australian longitudes and the subtropical jet wind speed becomes anomalously strong. By contrast, in the positive SAM phase, the subtropical jet stream wind speed anomalies weaken in eastern Australian longitudes and the zonal mid-latitude westerly winds contract polewards together with a more pronounced polar-front jet which is defined by an increase in mid-latitude zonal wind speed anomalies. Without any shift in latitude of either jet, there is a dipole in strength that oscillates between polar jet and subtropical jet, which does shift the storm track and associated baroclinic processes latitudinally. Both DJF and JJA reflect the annual anomalies in Fig. 6a, b for the same periods (see, Speer 2008). This negative phase SAM induced large scale circulation

regime, combined with the negative IPO induced circulation of a poleward shift in the subtropical ridge over the Tasman Sea/New Zealand longitudes, is responsible for the dominant rain-bearing synoptic-mesoscale low pressure systems that affected the NSW coast during the 1948–1975 period (Speer 2008). On the other hand, both positive MSLP and 300 hPa anomalies over eastern Australia from 1976 to 1998 (Fig. 7a, b, respectively), indicate a lack of mid-latitude/tropical tropospheric interaction. These positive annual anomalies for the period 1976–1998 are also reflected in the MSLP and 300 hPa circulation anomalies for both DJF and JJA and there has been little change to these positive circulation anomalies from 1998 to 2007 (Speer 2008).

In the mid-1970s to late 1990s high SOI 10–15 year variability (though not statistically significant at the 5% level—see Fig. 2c) is reinforced by high IPO (15 year) variability (Fig. 2a). So there are two possible explanations for reduced rainfall during the 1976–1998 period over the Australian subtropical east coast: (1) IPO induced positive MSLP anomalies from a northward displacement of the subtropical ridge (see Fig. 7a compared to Fig. 6a) and, (2) high SOI variability. However, it is questionable how much influence the SOI has on NSW coastal rainfall since, as mentioned previously, McBride and Nicholls (1983) found that the SOI is poorly correlated with rainfall along the NSW coastal strip.

Turning to the wavelet analyses of the four area-averaged rainfall regions (Fig. 3a–d), there is higher rainfall variability in the 1948–1975 negative or ‘cool’ IPO phase for CENSW and SENSW (SENSW in particular), than for SEQLD and NENSW. The reason for this difference is evident in the precipitable water and 850 hPa vector wind anomalies. High anomalous precipitable water in anomalous onshore airflow that penetrates inland is a feature in SENSW and CENSW but not in SEQLD or NENSW (see Fig. 6c, d). Hence both SENSW and CENSW benefitted from enhanced moisture advection from the adjacent marine boundary layer and enhanced orographic lifting resulting in higher precipitable water available for rain than SEQLD and NENSW. The reason for the larger SEQLD (Cape Morton) and NENSW (Yamba) coastal station rainfall variability than the SEQLD (Harrisville) and NENSW (Ebor) inland stations most likely relates to smaller mesoscale influences or seasonal differences and would need further investigation.

In the SAM wavelet analysis (Fig. 2b), apart from high 2–5 year variability in the 1970s and 1990s, there is evidence of high variability in the 15–30 year frequency band even though it lies outside the cone of influence. Currently, a lack of data restricts a monthly analysis of 15–30 year SAM periodicity prior to 1948 although seasonal and annual SAM reconstructions back to the late 1800s have

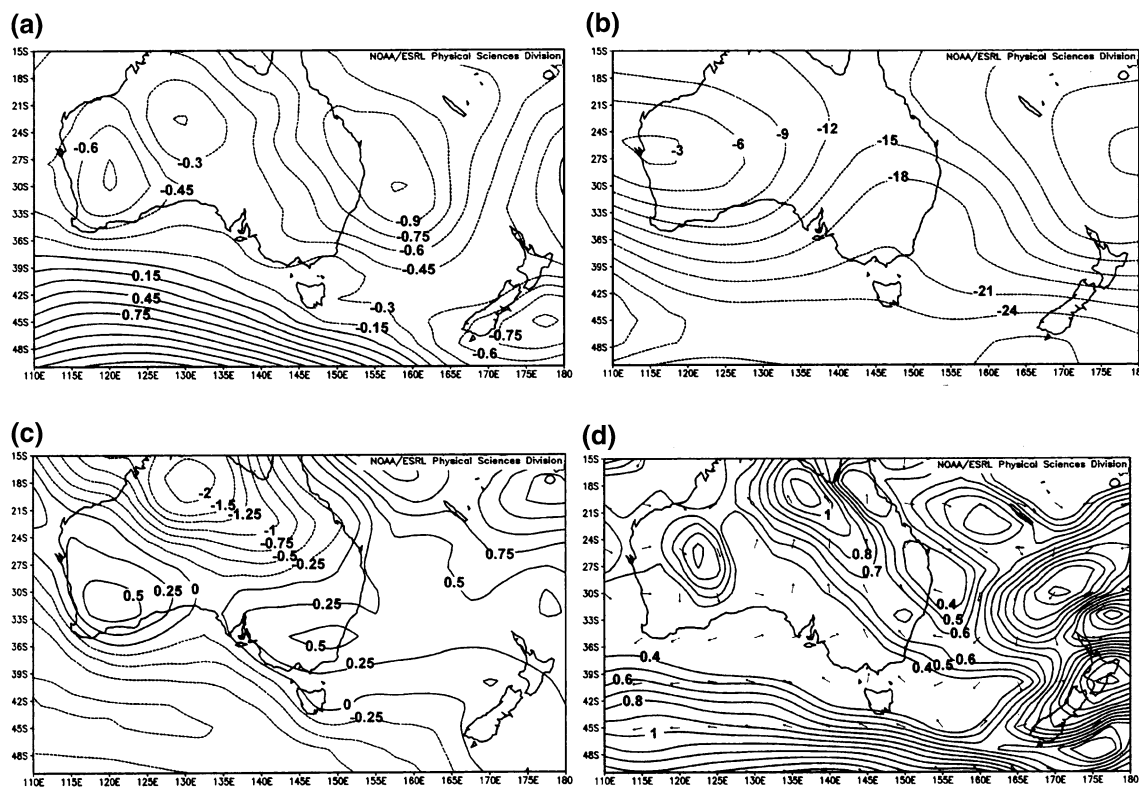


**Fig. 6** NCEP/NCAR composite atmospheric circulation anomalies over the Australian region from 1948 to 1975 for, (a) MSLP (hPa), (b) 300 hPa, (c) precipitable water ( $\text{kg m}^{-2}$ ), and (d) 850 hPa vector wind ( $\text{m s}^{-1}$ )

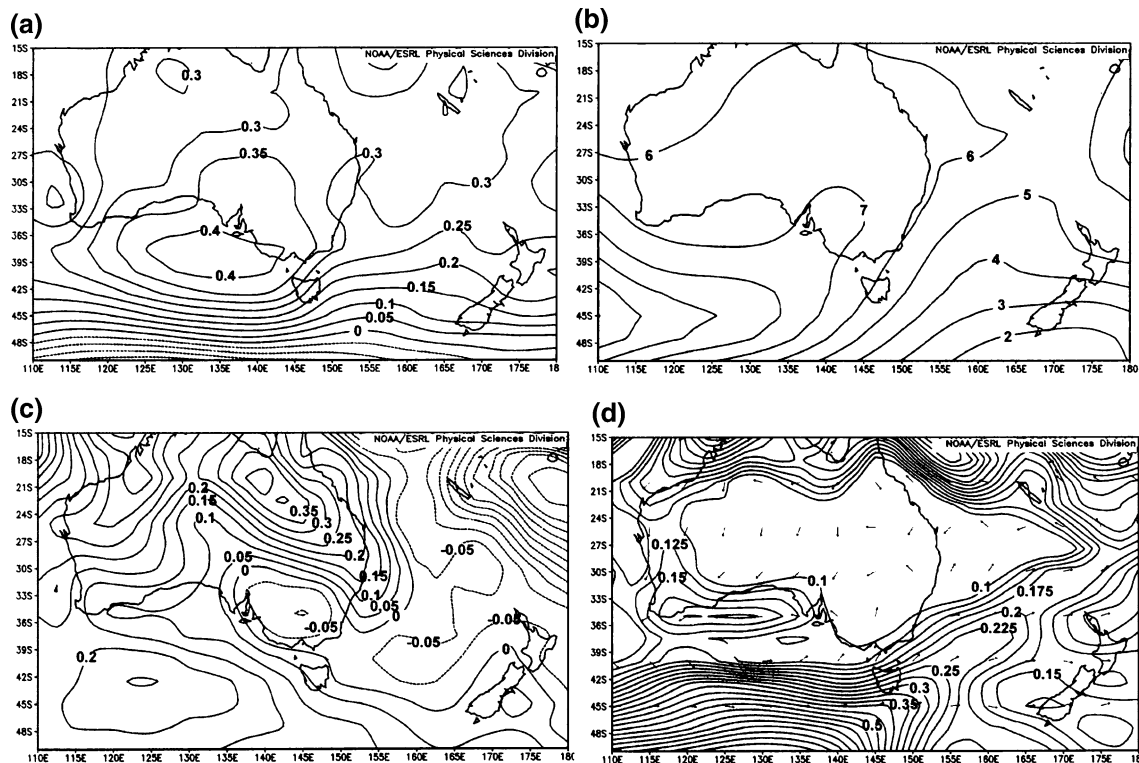


**Fig. 7** As in Fig. 6, except for 1976–1998

recently been completed (e.g., Visbeck 2009). The main feature on Fig. 2b is that the first high 15–30 year variability period ceased in the 1960s when the SAM was mostly negative and a second high variability period at 30 year periodicity commenced in the late 1990s when the SAM had become mostly positive. In terms of circulation anomalies the increasing positive SAM trend has not only led to the mid-latitude westerlies contracting poleward (Folland et al. 1999; Hendon et al. 2007; Meneghini et al. 2007; Rakich et al. 2008), but it also implies less chance for mid-latitude tropospheric troughs to interact dynamically with tropical moisture incursions into the subtropics, as occurred in the period 1948–1975 (see Fig. 6c, d). On the other hand, from 1976 to 1998 when SAM showed minimal decadal variability, the main influence in producing positive pressure anomalies over eastern Australia was the ‘warm’ phase of the IPO when the subtropical ridge shifted anomalously equatorward in the same area (see Fig. 7c, d). Since the late 1990s, SAM high 30 year variability has been the predominant, large scale atmospheric circulation influence producing positive pressure anomalies over eastern Australia (see Fig. 6a in Speer 2008). Marshall et al. (2004) conclude from GCM results that combined with natural forcings and ozone depletion, increases in greenhouse gases are an important component of the shift to more observed positive SAM values since the mid-1960s and, particularly, the austral summer.

#### 4 Summary and conclusions

Wavelet analyses of four area-averaged rainfall regions of Australia’s subtropical east coast, namely, SEQLD, NENSW, CENSW and SENSW, reveal periodicities of high rainfall variability in their global wavelet spectra over the period 1910–2007 that can be explained by three large scale climate drivers comprising the IPO, SAM and ENSO. While the annual cycle is a strong feature in SEQLD and NENSW rainfall variability, coastal stations in both these areas (Cape Morton and Yamba, respectively) also have high IPO (15–30 year periodicity) variability. For SENSW, the IPO periodicity in rainfall variability dominates, while CENSW represents a transition region between high annual periodicity further north and the dominant IPO periodicity in high variability for SENSW.

In confirmation of the rainfall decrease/large scale atmospheric climate driver relationships in this study, links have been made to characteristics of rain-bearing weather systems that affect parts of Australia’s subtropical east coast and three large scale atmospheric climate drivers. A step decrease in coastal rain-bearing low pressure systems on the Australian subtropical east coast has been linked to a change in phase of the IPO from negative (cool) to positive

(warm) in the mid-1970s. The rainfall decline in the southeast of NSW has been linked to an increasing positive SAM trend that contracts the mid-latitude westerlies poleward, while the rainfall decrease in the northern most part of the study area has been most influenced by ENSO through a predominance of El Niño conditions during the ‘warm’ IPO phase (1976–1998). Furthermore, both during this period and since 1998 the poleward contraction of the mid-latitude westerlies south of Australia has greatly reduced the possibility of tropical-midlatitude tropospheric interaction over the subtropical coast of eastern Australia. For increased interaction to occur, as it did during the previous cool phase of the IPO, low level tropospheric circulation anomalies in pressure (negative) and moisture (positive) need to occur over eastern Australia with the subtropical ridge located anomalously poleward. However, from 1998 to 2007 the mostly positive SAM, resulting from poleward contracted, enhanced mid-latitude westerlies, has been a dominant influence preventing this from occurring.

Both the IPO in this study and the SAM in this and previous work (e.g., Hendon et al. 2007; Meneghini et al. 2007; Speer 2008) are shown to have an important controlling influence on Australian subtropical east coast rainfall on multi-decadal time scales and further work in developing these relationships in this highly populated area of Australia would enhance our knowledge of rainfall variability on seasonal to multi-decadal timescales. Future work will include analyzing global SST relationships with large scale climate drivers and Australian east coast rainfall.

**Acknowledgments** This work was financially supported through the Australian Academy of Science under the Scientific Visits to North America program. Wavelet software was provided by C. Torrence and G. Compo, and is available at URL: <http://paos.colorado.edu/research/wavelets/>.

#### References

- Ansell TJ, Reason CJC, Smith IN, Keay K (2000) Evidence for decadal variability in southern Australian rainfall and relationships with regional pressure and sea surface temperature. *Int J Climatol* 20:1113–1129
- Bureau of Meteorology (2005) El Niño, La Niña and Australia’s Climate. Bureau of Meteorology, Melbourne
- Bureau of Meteorology (2006) An exceptionally dry decade in parts of southern—and eastern Australia: October 1996 to September 2006. Special Climate Statement 9, 10 October 2006, National Climate Centre, Bureau of Meteorology, Australia
- Chen J, Del Genio AD, Carlson BE, Bosilovich MG (2008) The spatiotemporal structure of twentieth-century climate variations in observations and reanalyses. Part I: long-term trend. *J Clim* 21:2611–2633
- Codron F (2005) Relation between annular modes and the mean state: southern hemisphere summer. *J Clim* 18:320–330

- Codron F (2007) Relations between annular modes and the mean state: southern hemisphere winter. *J Atmos Sci* 64:3328–3339
- Cordery I, Opoku-Ankomah Y (1994) Temporal variation of relations between tropical sea-surface temperatures and New South Wales rainfall. *Aust Meteorol Mag* 43:73–80
- Folland CK, Parker DE, Colman AW, Washington R (1999) Large scale modes of ocean surface temperature since the late nineteenth century. In: Navarra A (ed) Beyond El Niño: decadal and interdecadal climate variability. Springer, The Netherlands, pp 73–102
- Foufoula-Georgiou E, Kumar P (eds) (1995) Wavelets in geophysics. Academic Press, New York, p 373
- Hendon HH, Thompson DWJ, Wheeler MC (2007) Australian rainfall and surface temperature variations associated with the southern annular mode. *J Clim* 20:2452–2467
- Hope P (2005) Reanalysis datasets and potential problems. In: Indian Ocean climate initiative stage 2: unabridged reports of phase 1 activity. [http://www.ioci.org.au/publications/pdf/IOCI\\_Stage2\\_UnabridgedReports\\_Phase1Theme1.pdf](http://www.ioci.org.au/publications/pdf/IOCI_Stage2_UnabridgedReports_Phase1Theme1.pdf)
- Jones DA, Weymouth GT (1997) An Australian monthly rainfall dataset. Technical Report no. 70 Bureau of Meteorology, Australia
- Kalnay et al (1996) The NCEP/NCAR 40-year reanalysis project. *Bull Am Meteorol Soc* 77:437–471
- Kestin TS, Karoly DJ, Yano I, Rayner NA (1998) Time-frequency variability of ENSO and stochastic simulations. *J Clim* 11:2258–2272
- Kidston J, Renwick JA, McGregor J (2009) Hemispheric scale seasonality of the southern annular mode and impacts on the climate of New Zealand. *J Clim* (in press)
- Lau KM, Wen H (1995) Climate signal detection using wavelet transform: how to make a time series sing. *Bull Am Meteorol Soc* 76:2391–2402
- Lavery B, Joung G, Nicholls N (1997) An extended high-quality historical rainfall dataset for Australia. *Aust Meteorol Mag* 46:27–38
- Mantua NJ, Hare SR, Zhang Y, Wallace JM, Francis RC (1997) A Pacific interdecadal climate oscillation with impacts on salmon production. *Bull Am Meteorol Soc* 78:1069–1079
- Marshall GJ, Stott PA, Turner J, Connelley WM, King JC, Lachlan-Cope TA (2004) Causes of exceptional atmospheric circulation changes in the Southern Hemisphere. *Geophys Res Lett* 31:L14205. doi:[10.1029/2004GL019952](https://doi.org/10.1029/2004GL019952)
- McBride JL, Nicholls N (1983) Seasonal relationships between Australian rainfall and the Southern Oscillation. *Mon Weather Rev* 111:1998–2004
- Meneghini B, Simmonds I, Smith IN (2007) Association between Australian rainfall and the southern annular mode. *Int J Climatol* 27:109–121
- Morlet J (1982) Wave propagation and sampling theory. *Geophysics* 47:222–236
- Murphy BF, Timbal B (2008) A review of recent climate variability and climate change in southeastern Australia. *Int J Climatol* 28:859–879
- Nan S, Li J (2003) The relationship between summer precipitation in the Yangtze River valley and the previous Southern Hemisphere annular mode. *Geophys Res Lett* 30(24):2266
- Nicholls N (2006) Detecting and attributing Australian climate change: a review. *Aust Meteorol Mag* 55:199–211
- Nicholls N (2009) Local and remote causes of the southern Australian autumn–winter rainfall decline, 1958–2007. *Clim Dyn*. doi:[10.1007/s00382-009-0527-6](https://doi.org/10.1007/s00382-009-0527-6)
- Nicholls N, Kariko A (1993) East Australian rainfall events: interannual variations, trends, and relationships with the Southern Oscillation. *J Clim* 6:1141–1152
- Parker D, Folland C, Scaife A, Knight J, Colman A, Baines P, Dong B (2007) Decadal to multidecadal variability and the climate change. *J Geophys Res* 112:D18115. doi:[10.1029/2007JD008411](https://doi.org/10.1029/2007JD008411)
- Pezza AB, Simmonds I, Renwick JA (2007) Southern Hemisphere cyclones and anticyclones: recent trends and links with decadal variability in the Pacific Ocean. *Int J Climatol* 27:1403–1419
- Power S, Casey T, Folland C, Colman A, Mehta V (1999) Inter-decadal modulation of the impact of ENSO on Australia. *Clim Dyn* 15:319–324
- Power S, Haylock M, Colman R, Wang X (2006) The predictability of interdecadal changes in ENSO activity and ENSO teleconnections. *J Clim* 19:4755–4771
- Rakich C, Holbrook NJ, Timbal B (2008) A pressure gradient metric capturing planetary-scale influences on eastern Australian rainfall. *Geophys Res Lett* 35:L08713
- Rayner NA, Brohan P, Parker DE, Folland CK, Kennedy JJ, Vanicek M, Ansell TJ, Tett SFB (2006) Improved analyses of changes and uncertainties in sea surface temperature measured in situ since the mid-nineteenth century: the HadSST2 dataset. *J Clim* 19:446–469. doi:[10.1175/JCLI3637.1](https://doi.org/10.1175/JCLI3637.1)
- Salinger MJ, Renwick JA, Mullan AB (2001) Interdecadal Pacific Oscillation and South Pacific climate. *Int J Climatol* 21:1705–1721
- Speer MS (2008) On the late twentieth century decrease in Australian east coast rainfall extremes. *Atmos Sci Lett* 9:160–170
- Stone R, Auliciems A (1992) SOI phase relationships with rainfall in eastern Australia. *Int J Climatol* 12:625–636
- Thompson DWJ, Wallace JM (2000) Annular modes in the extratropical circulation. Part I: month-to-month variability. *J Clim* 13:1000–1016
- Torre C, Compo GP (1998) A practical guide to wavelet analysis. *Bull Am Meteorol Soc* 79(1):61–78
- Torre C, Webster PJ (1999) Interdecadal changes in the ENSO–monsoon system. *J Clim* 12:2679–2690
- Ummenhofer CC, England MH, McIntosh PC, Meyers GA, Pook MJ, Risbey JS, Sen Gupta A, Taschetto AS (2009) What causes Southeast Australia's worst droughts? *Geophys Res Lett* 36:L04706. doi:[10.1029/2008GL036801](https://doi.org/10.1029/2008GL036801)
- Visbeck M (2009) A station-based southern annular mode index from 1884 to 2005. *J Clim* 22:940–950
- Zhang X-G, Casey TM (1992) Long-term variations in the Southern Oscillation and relationships with Australian rainfall. *Aust Meteorol Mag* 40:211–225
- Zhang Y, Wallace JM, Battisti DS (1997) ENSO-like interdecadal variability: 1900–93. *J Clim* 10:1004–1020